

I. INTRODUCTION

AdS/CFT correspondence, also known as gauge-gravity duality is one of the most exciting discoveries in modern theoretical physics. This correspondence adapted to describe the low-energy dynamics of QCD in the simplest models known as AdS/QCD models. These models are useful for understanding properties of QCD at low energies such as chiral symmetry breaking, hidden local symmetry, vector meson dominance at large N and high energy regimes. There are two approaches in AdS/QCD correspondence the top-down and bottom-up approaches [1]. The first one gives low-energy hadron properties and models of this approach based on the D -brane constructions in string theory. The bottom-up approach describes various low-energy phenomenology of QCD. Directly applying the AdS/CFT correspondence between the boundary gauge field theory and bulk gravity the hard and soft-wall models are the typical ones in the bottom-up approaches. Mass spectra, decay and coupling constants, form factors are calculated in the framework of these models. Holographic QCD models are useful as well as for the study of internal structure of hadrons, including their excitations by means of study of the transition form factors. Electromagnetic transition form factors of nucleons were studied in the light-front holographic QCD in Refs. [2–4], also, within the soft-wall model in Refs. [5, 6].

Here, we aim to consider the $N + \gamma^* \rightarrow R(1440, 1535, 1710)$ transitions form factors for the Roper resonance, which may have the positive or negative parity, in the framework of the hard-wall model. These transitions were studied in Refs. [5, 6] within the soft-wall model at the finite and zero temperature cases.

This paper is structured as follows: We introduce the profile function for the nucleons in Sec. II and briefly discuss the electromagnetic current and form factors in Secs. III and IV accordingly. In Sec. V, we discuss the form factors of the $N + \gamma^* \rightarrow R(1440, 1535, 1710)$ transitions. Finally, in Sec. VI, we present our numerical analysis and results.

II. NUCLEONS IN HARD-WALL MODEL

Electromagnetic transition form factors are an important probe for the study of the internal structure of nucleons. These form factors were studied in the framework of certain models. We apply the hard-wall model of the holographic QCD for the calculation of these Roper-nucleon transition form factors. To this end, firstly, we introduce nucleons and briefly present the known formulas for a description of these particles in this model. The metric for this model is the five-

dimensional AdS metric in Poincare patch:

$$ds^2 = \frac{1}{z^2}(\eta_{\mu\nu}dx^\mu dx^\nu - dz^2). \quad (2.1)$$

The fifth coordinate z extends from 0 to ∞ . These boundaries of the AdS space are called the ultraviolet (UV) and infrared (IR) ones, respectively. $\eta_{\mu\nu}$ is the metric of the Minkowski space ($\eta_{\mu\nu} = \text{diag}(1, -1, -1, -1)$; $\mu, \nu = 0, 1, 2, 3$).

As is known from [19], in order to describe nucleons in the AdS/CFT correspondence framework, it is necessary to introduce two independent fermion fields in the bulk of AdS space, which describe to chiral components of the nucleons. The minimal bulk action for the spinor field is written in the following:

$$S = \int dz d^4x \sqrt{g} (i\bar{N}_1 e_A^M \Gamma^A D_M N_1 - m_5 \bar{N}_1 N_1), \quad (2.2)$$

where g -is the determinant of the AdS metric, e_A^M is the vielbein for the metric (2.1) and $\Gamma^A = (\gamma^\mu, -i\gamma^5)$ are the Dirac matrices. The Lorentz and gauge-covariant derivative is defined in the below form:

$$D_M = \partial_M - \frac{i}{4} \omega_M^{AB} \Sigma_{AB}, \quad (2.3)$$

where ω_M^{AB} is the spin connection and Σ_{AB} is defined as: $\Sigma_{AB} = \frac{1}{2i}[\Gamma^A, \Gamma^B]$. Nonvanishing components of the spin connections for the metric (2.1) are the following ones $\omega_\mu^{5A} = -\omega_\mu^{A5} = \frac{1}{z}\delta_\mu^A$. Equation of motion obtained from the action (2.2) has an explicit form:

$$(z\gamma^5\partial_z + iz\not{\partial} - 2\gamma^5)N_1 - m_5N_1 = 0. \quad (2.4)$$

It is favorable to solve this equation in terms of Fourier components:

$$N_{1,2} = \frac{1}{2\pi} \int [F_{1,2L}(p, z)\psi_{1,2L}(p) + F_{1,2R}(p, z)\psi_{1,2R}(p)] e^{-ipx} d^4p, \quad (2.5)$$

were the 4D spinors satisfy the free Dirac equation:

$$\not{p}\Psi(p) = |p|\Psi(p). \quad (2.6)$$

Here p denotes $p = |p| = \sqrt{p^2}$ for a time-like four-momentum p . Then the Dirac equation (2.4) will be written as equations for the profile functions $F_{1,2L,R}$:

$$\begin{aligned} \left(-\frac{4}{z}\partial_z + \frac{6 + m_5 - m_5^2}{z^2}\right) F_{1,2L}(pz) &= -p^2 F_{1,2L}(pz), \\ \left(-\frac{4}{z}\partial_z + \frac{6 + m_5 - m_5^2}{z^2}\right) F_{1,2R}(pz) &= -p^2 F_{1,2R}(pz). \end{aligned} \quad (2.7)$$

Extra components of these spinors are eliminated by the UV and IR boundary conditions [9, 10] imposed on the $N_{1,2}$ spinors. The mass eigenvalues of the Kaluza-Klein modes depend on which profile vanishes at the IR boundary $F_R(z_0) = 0$. Solutions to the equations (2.7) are expressed in terms of Bessel functions $J_{2,3}$ [11, 12]:

$$\begin{aligned} F_{1L}^n(pz) &= -c_1^n z^{\frac{5}{2}} J_2(pz), F_{1R}^n(pz) = c_1^n z^{\frac{5}{2}} J_3(pz), \\ F_{2L}^n(pz) &= -c_2^n z^{\frac{5}{2}} J_3(pz), F_{2R}^n(pz) = c_2^n z^{\frac{5}{2}} J_2(pz), \end{aligned} \quad (2.8)$$

where $c_{1,2}^n$ are constants were found from the normalization conditions and are equal [12]:

$$|c_{1,2}^n| = \frac{\sqrt{2}}{z_m J_2(M_n z_m)}. \quad (2.9)$$

Here, M_n is the mass spectrum of the Kaluza-Klein modes corresponding to the ground and excited states of the boundary nucleons. This spectrum M_n is expressed in terms of zeros $\alpha_n^{(3)}$ of the Bessel function J_3 :

$$M_n = \frac{\alpha_n^{(3)}}{z_m}. \quad (2.10)$$

III. VECTOR FIELD

Action for the 5-dimensional vector field V_M corresponding to the photon field in the boundary theory is written in the form:

$$S_V = -\frac{1}{2g_5^2} \int d^5x \sqrt{g} Tr F_{MN}^2, \quad (3.1)$$

where $F_{MN} = \partial_M V_N - \partial_N V_M$ up to motion quadratic order in the action. The usual gauge fixing of the V_z component is the axial gauge $V_z = 0$. Fourier transform of the vector field V_μ will be written as [13]:

$$V_\mu(x, z) = \int \frac{d^4q}{(2\pi)^4} e^{-iqx} V_\mu(q) V(q, z), \quad (3.2)$$

where the bulk-to-boundary propagator $V(q, z)$ obeys the equation of motion

$$\partial_z \left(\frac{1}{z} \partial_z V(q, z) \right) + \frac{q^2}{z} V(q, z) = 0, \quad (3.3)$$

obtained from the action (3.1) and imposed the boundary conditions $V(q, \epsilon) = 1$ and $\partial_z V(q, z_0) = 0$. $V_\mu(q)$ is the UV boundary value of the free vector field. The solution of the equation (3.3) is written in terms of the Bessel function [14, 15]:

$$V(q, z) = \frac{\pi}{2} z q \left(\frac{Y_0(qz_0)}{J_0(q, z_0)} J_1(qz) - Y_1(qz) \right). \quad (3.4)$$

Note that the vector field function $V_\mu(q)$ is the source for the nucleon current $J_\mu^a = \bar{N} \gamma_\mu t^a N$.

IV. TRANSITION CURRENT FORM FACTORS AND HELICITY AMPLITUDES

Electromagnetic transition form factors are a source of information about the internal structure of nucleons and other hadrons. These form factors for the nucleon to R transition have been studied in several theoretical approaches. The electromagnetic form factors of the $N + \gamma^* \rightarrow R$ transition are defined due to Lorentz and gauge invariance of the interaction by the following matrix element [17, 18]:

$$M^\mu(p_1, \lambda_1, p_2, \lambda_2) = \bar{u}(p_1, \lambda_1) [\gamma_\perp^\mu F_1(Q^2) + i\sigma^{\mu\nu} \frac{q_\nu}{M} F_2(Q^2)] u(p_2, \lambda_2), \quad (4.1)$$

where $\bar{u}(p_1, \lambda_1)$ and $u(p_2, \lambda_2)$ are the spinors describing the R resonance and the nucleon, respectively. M is the sum of the nucleon and Roper nucleon masses ($M = M_N + M_R$ for the $N + \gamma^* \rightarrow R(1440)$; $M = \frac{M_N + M_R}{2}$ for $N + \gamma^* \rightarrow R(1710)$), $\gamma_\perp^\mu = \gamma^\mu - q^\mu \frac{q}{q^2}$, $q = p_1 - p_2$. The final and initial baryons helicities (λ, λ_1) are related with the $\lambda_2 = \lambda_1 - \lambda$ photon helicity. The four-momenta of Roper, nucleon, photon and the polarization vector of a photon are specified as [19, 20]:

$$p_1 = (M_1, \vec{0}), p_2^\mu = (E_2, 0, 0, -|P|), q^\mu = (q^0, 0, 0, |p|) \quad (4.2)$$

$$\epsilon^\mu(\pm) = (0, \vec{\epsilon}^\pm), \vec{\epsilon}^\pm = \frac{1}{\sqrt{2}}(\pm 1, i, 0) \quad (4.3)$$

$$\epsilon^\mu(0) = \frac{1}{\sqrt{Q^2}}(|p|, 0, 0, q^0) \quad (4.4)$$

where, $E_2 = \frac{Q_+}{2M_R} - M_N$, $Q_\pm = M_\pm^2 + Q^2$, $Q^2 = -q^2$, $M_\pm = M_R \pm M_N$ and $|p| = \frac{\sqrt{Q_+ Q_-}}{2M_R}$ is the value of the three-momentum of the nucleon or the photon. The electromagnetic current of the Roper-nucleon transitions are defined as follows [21–24]:

$$J^\mu = \bar{u}_f(P_f) [\gamma_\mu^T F_1^{fi}(Q^2) + \frac{1}{m_{fi}} \sigma_{\mu\nu} Q_\nu F_2^{fi}(Q^2)] u_i(P_i). \quad (4.5)$$

Here $P_{i,f}$ are incoming/outgoing nucleons have four-momenta and masses $m_{i,f}$ so that $P_{i,f}^2 = m_{i,f}^2$; $Q = P_f - P_i$; $m_{fi} = (m_f + m_i)$, $F_{1,2}$ are called Dirac and Pauli form factors, respectively.

V. DIRAC AND PAULI FORM FACTORS. HELICITY AMPLITUDES

A. Form factors

In order to obtain form factors of $R \rightarrow N$ transitions within the holographic QCD, we have to write an action for the bulk interaction between the fields, which is defined as:

$$S_{int} = \int d^4x dz \sqrt{g} L_{int}(x, z). \quad (5.1)$$

Here $L_{int}(x, z)$ is the Lagrangian of the interaction between the spinor and vector fields [5, 18]:

$$L_{int}(x, z) = \sum c_\tau^{RN} \bar{\Psi}_{i,\tau}^R(x, z) \hat{V}_i(x, z) \Psi_{i,\tau}^N(x, z). \quad (5.2)$$

Here c_τ are the mixing parameters that contribute of the AdS fermion fields with different twist dimension [18]. $\bar{V}_\pm(x, z)$ denotes :

$$\bar{V}_\pm(x, z) = \tau_3 \Gamma^M V_M(x, z) \pm \frac{i}{4} \eta_V [\Gamma^M, \Gamma^N] V_{MN}(x, z) \pm g_V \tau_3 \Gamma^M i \Gamma^z V_M(x, z). \quad (5.3)$$

Here τ_3 is the isospin Pauli matrix, η_V is the matrix of the η_p, η_n coupling constants:

$$\eta_V = \text{diag}(\eta_p, \eta_n). \quad (5.4)$$

$V_{MN} = \partial_M V_N - \partial_N V_M$ is the stress tensor of the vector field. After taking into account the definitions (5.2), (5.3) in (5.1), we obtain the following expression for the action in the momentum representation:

$$\begin{aligned} S_{int} = \int \int \frac{dz}{z^5} d^4p d^4p' V(q, z) V_\mu(q) & \left[\frac{cz}{2} [F_L^*(z) F_L(z) + F_R^*(z) F_R(z) + F_R^*(z) F_R(z) \right. \\ & - F_L^*(z) F_L(z)] \bar{u}(p') \gamma^\mu u(p) - \eta_V z^2 q_\nu [F_R^*(z) F_R(z) - F_L^*(z) F_L(z) \\ & \left. - F_R^*(z) F_L(z) - F_L^*(z) F_R(z)] \bar{u}(p') \sigma^{\mu\nu} u(p) \right]. \quad (5.5) \end{aligned}$$

Here $|p| = M_{nuc}$, $|p'| = M_{Rop}$ and $q_\nu = p - p'$. The profile functions $F_{L,R}^*(|p'|z)$ and $F_{L,R}(|p|z)$ describe the Roper state and nucleon, respectively. According to AdS/CFT correspondence of the bulk and boundary theories the generating functionals of the gauge and AdS gravity theories are equivalent:

$$Z_{gauge} = Z_{AdS}. \quad (5.6)$$

The vector current of nucleons, which is defined in the QCD theory, can be calculated from the Z_{AdS} using the correspondence equality (5.6). Generating function Z_{AdS} is defined as an exponent of classical bulk action S_{int} :

$$Z_{AdS} = e^{iS_{int}}. \quad (5.7)$$

The vacuum expectation value of the nucleon's vector current J_μ in the boundary QCD theory will be found applying the holographic formula:

$$\langle J_\mu \rangle = -i \frac{\delta Z_{QCD}}{\delta V_\mu(q)} \Big|_{V_\mu=0} = -i \frac{\delta e^{iS_{int}}}{\delta V_\mu(q)} \Big|_{V_\mu=0}. \quad (5.8)$$

From the comparison the electromagnetic current of the Roper-nucleon transitions (4.5) with the nucleon vector current (5.9) for the $Q^2 = -q^2 > 0$ momentum transfer the $G_i(Q^2)$ form factors will be written in terms of integrals over the z variable:

$$G_1(Q^2) = \frac{1}{2} \int_0^{z_m} dz V(Q, z) \sum_\tau c_\tau^{RN} (F_{\tau,0}^L(z) F_{\tau,1}^L(z) + F_{\tau,0}^R(z) F_{\tau,1}^R(z)), \quad (5.9)$$

$$G_2(Q^2) = \frac{1}{2} \int_0^{z_m} dz V(Q, z) \sum_\tau c_\tau^{RN} (F_{\tau,0}^R(z) F_{\tau,1}^R(z) - F_{\tau,0}^L(z) F_{\tau,1}^L(z)), \quad (5.10)$$

$$G_3(Q^2) = \frac{1}{2} \int_0^{z_m} dz \partial_z V(Q, z) \sum_\tau c_\tau^{RN} (F_{\tau,0}^L(z) F_{\tau,1}^L(z) - F_{\tau,0}^R(z) F_{\tau,1}^R(z)), \quad (5.11)$$

$$G_4(Q^2) = \frac{M}{2} \int_0^{z_m} dz V(Q, z) \sum_\tau c_\tau^{RN} (F_{\tau,0}^L(z) F_{\tau,1}^R(z) + F_{\tau,1}^L(z) F_{\tau,0}^R(z)). \quad (5.12)$$

The Dirac and Pauli form factors $F_1(Q^2)$ and $F_2(Q^2)$ are defined by means of the G_i form factors in the following [25, 26]:

$$F_1(Q^2) = G_1(Q^2) + g_V G_2(Q^2) + \eta_V G_3(Q^2), \quad (5.13)$$

$$F_2(Q^2) = \eta_V G_4(Q^2) \quad (5.14)$$

The $F_{1,2}$ form factors are normalized to the electric charge e_N and anomalous magnetic moment μ_a of the nucleon: $F_1(0) = e_N$ and $F_2(0) = \mu_a = g(e/2M) = 1.79\mu_B$. A point particle of charge e and total magnetic moment $(g+1)\mu_B$ is a particle for which $F_1(Q^2) = e$ and $F_2(Q^2) = g\mu_B$ for all values of Q^2 . Thus by definition, a particle has an electromagnetic structure-i.e. is not a point particle-if and only if the functions $F_1(Q^2)$ and $F_2(Q^2)$ are not constant. The functions F_1 and F_2 are called the charge and moment form factors of the nucleon, respectively.

B. Helicity amplitudes

In addition to the electromagnetic transition form factors the $A_{1/2}$ and $S_{1/2}$ helicity amplitudes are defined through the transition matrix element of the transverse electromagnetic interaction between the nucleon and the Roper resonance states:

$$A_{1/2}(Q^2) = \sqrt{\frac{2\pi\alpha}{K}} \left\langle R, S'_z = +\frac{1}{2} \mid \varepsilon_+ J \mid N, S_z = -\frac{1}{2} \right\rangle, \quad (5.15)$$

$$S_{1/2}(Q^2) = \sqrt{\frac{2\pi\alpha}{K}} \left\langle R, S'_z = +\frac{1}{2} \mid \varepsilon_0 J \mid N, S_z = -\frac{1}{2} \right\rangle \frac{|q|}{Q}, \quad (5.16)$$

where q is the photon three-momentum in the rest frame of nucleons, ε_λ^μ ($\lambda = 0, \pm 1$) is the photon polarization vector, $\alpha \simeq 1/137$ is the fine-structure constant, $K = |q| = \frac{M_R^2 - M_N^2}{2M_R}$. The magnitude of the photon three-momentum is defined

$$|\mathbf{q}| = \frac{\sqrt{Q_+^2 Q_-^2}}{2M_R}, \quad (5.17)$$

where $Q_\pm = (M_R \pm M_N)^2 + Q^2$. Note that when $Q^2 = 0$, one has $K = |q| = \frac{M_R^2 - M_N^2}{2M_R}$, as made note above. For the $N + \gamma^* \rightarrow R(1535)$ transition, where Roper state is the $J^P = -1/2$ state, the $A_{1/2}$, $S_{1/2}$ helicity amplitudes are written in terms of the Pauli and Dirac form factors [35, 36]:

$$A_{1/2}(Q^2) = 2A_R [F_1(Q^2) + \frac{M_R - M_N}{M_R + M_N}] F_2(Q^2), \quad (5.18)$$

$$S_{1/2}(Q^2) = -\sqrt{2} A_R (M_R + M_N) \frac{|q|}{Q^2} \left[\frac{M_R - M_N}{M_R + M_N} F_1(Q^2) - \tau F_2(Q^2) \right]. \quad (5.19)$$

here $A_R = \frac{e}{4} \sqrt{\frac{Q_+^2}{M_N M_R K}}$. For the $N + \gamma^* \rightarrow R(1440, 1710)$ transitions the $A_{1/2}$, $S_{1/2}$ amplitudes have forms [33, 34]:

$$A_{1/2}(Q^2) = R [F_1(Q^2) + \frac{M_R - M_N}{M_R + M_N}] F_2(Q^2), \quad (5.20)$$

$$S_{1/2}(Q^2) = \frac{R}{\sqrt{2}} |q| \frac{M_R + M}{Q^2} (F_1(Q^2) - \tau F_2(Q^2)), \quad (5.21)$$

where τ and R denote: $\tau = \frac{Q^2}{(M_R + M)^2}$, $R = \sqrt{\frac{\pi\alpha Q_-^2}{M_R M K}}$.

VI. NUMERICAL ANALYSIS

We carry out the numerical calculations for the $F_{1,2}$ form factors according to the (5.13) and (5.14) formulas. The parameters and constants in these formulas are fixed as $c_3^{RN} = 0.72$, $\eta_p = 0.453$ [5], $z_m = \frac{1}{\Lambda_{QCD}} = 0.205 \text{ GeV}$.

In Fig.1, we present our form factors numerical results for the $N + \gamma^* \rightarrow R(1440)$ electromagnetic transition. We compare our results with the CLAS [32], MAID [37] experimental data and valence quark contributions model [33]. As is seen from the figure, in the $1 \leq Q^2 \leq 5 \text{ GeV}$ interval our results are close to the data from CLAS and MAID experiments. In Fig.2 we compare our results to CLAS, MAID experimental data and valence quark model contributions for the $A_{1/2}$ and

$S_{1/2}$ helicity amplitudes for this transition. It is noticeable that for this transition, the hard-wall model results for the $S_{1/2}(Q^2)$ amplitude are in good noticeable agreement with the results of the CLAS and MAID experiments.

In Fig.3 we plot graphs for the $F_{1,2}(Q^2)$ form factors for the $N+\gamma^* \rightarrow R(1535)$ transition, where the Roper state has negative parity, and compare our graphs to the results of the semirelativistic approximation [4], CLAS [32], JLab/Hall C [36] and MAID [34, 35] experimental data. For this transition our results are in a good agreement with the experimental datas. In Fig.4 we plot the $A_{1/2}$ and $S_{1/2}$ helicity amplitudes. The hard-wall results for the helicity amplitudes differ from the experimental data for this transition.

The form factor results for the $N + \gamma^* \rightarrow R(1710)$ transition are presented in Fig.5 and compared with the nonrelativistic quark model [7] and the data from CLAS [32], MAID [37] experiments. Our results for the Pauli and Dirac form factors are close to these experimental data. The hard-wall results for the $A_{1/2}$ and $S_{1/2}$ helicity amplitudes for this transition are given in Fig.6. The graphs of these amplitudes are close to the experimental data at some points.

VII. CONCLUSION

We apply the hard-wall model for the nucleon-Roper transition form factors investigation and consider the $N + \gamma^* \rightarrow R(1440), R(1535), R(1710)$ transitions. We also check this model for the helicity amplitudes study in these transition cases. As is seen from the comparison of the graphs, the holographic hard-wall model gives good results for some form factor and helicity amplitude behaviours, though in other cases, only some points are close to the experimental data.

-
- [1] A. B. Santra, U. Lombardo, A. Bonanno, Journal of Physics: Conference Series 374 (2012) 012004.
 - [2] G. Ramalho, D. Melkinov, J. M. Maldacena, ITEP-TH-08/17, (2017) [arXiv:1703.03819v1 [hep-ph]].
 - [3] G. Ramalho, LFTC-17-9/9, 22 Sep. 2017 [arXiv:1706.05707v2-[hep-ph]] .
 - [4] G. Ramalho, LFTC-17-9/9, 14 Mar. 2017 [arXiv:1612.09555v2-[hep-ph]].
 - [5] T. Gutsche, V. E. Lyubovitskij, I. Schmidt, A. Vega, Phys. Rev. D **87**, 016017 (2013) [arXiv:1212.6252[hep-ph]].
 - [6] Th. Gutsche, V. E. Lyubovitskij, I. Schmidt, Nucl. Phys. B **952** (2020) 114934.
 - [7] G. Ramalho, K. Tsushima, 31 Mar. 2014 [arXiv:1402.3234v2 [hep-ph]] .
 - [8] I. G. Aznauryan, A. Bashir, V. Braun, S. J. Brodsky, V. D. Burkert, L. Chang, C. Chen and B. El Ben- nich et al., Int. J.Mod.Phys. E, **22**, 1330015(2013), [arXiv:1212.4891 [nucl-th]].

- [9] D. K. Hong, T. Inami and H. U. Yee Phys. Lett. B **646**, 165(2007), [arxiv:hep-ph/0609270].
- [10] V. I. Mokeev et al. [CLAS Collaboration]. Phys. Rev. C **86**,035203 (2012), [arXiv:1205.3948[nucl-ex]].
- [11] D. K. Hong, T. Inami and H. U. Yee, PNUTP-06/A20, KIAS-P06040,[arxiv:0609270v2[hep-ph]].
- [12] N. Maru, M. Tachibana Eur. Phys. J.C **63**, 123 (2009), [arXiv:0904.3816[hep-ph]].
- [13] Th. Gutsche,V. E. Lyubovitskij I. Schmidt, Phys. Rev. D **97**, 054011(2018).
- [14] H. R. Grigoryan and A. V. Radyushkin, Phys. Lett. B **650**, 421 (2007), [arxiv:0703069v2[hep-ph]].
- [15] Zainul Abidin, Carl E. Carlson, 28 Jan 2008 [arXiv:0801.3839v2 [hep-ph]].
- [16] T. Gutsche, V. E. Lyubovitskij, I. Schmidt, A. Vega, Phys. Rev. D **87**, 016017(2013).
- [17] C. Alexandrou, M. Brinet, J. Carbonell, M. Constantinou, 10 Feb. 2011 [arXiv:1102.2208v1[hep-lat]].
- [18] Th. Gutsche, V. E. Lyubovitskij and I. Schmidt, 25 Dec. 2017 [arXiv:1712.08410v2 [hep-ph]].
- [19] H. J. Weber, Phys. Rev. C **41**, 2783 (1990).
- [20] L. Tiator and M. Vanderhaeghen, Phys. Lett. B **672**, 344 (2009) [arXiv:0811.2285[hep-ph]].
- [21] G. Ramalho, M. T. Pena, 20 May 2014 [arXiv:1309.0730v2 [hep-ph]].
- [22] S. Dagaonkar, P. Jain, [arXiv:1503.06938v1 [hep-ph]].
- [23] D. J. Wilson, I. C. Cloet, L. Chang and C. D. Roberts, 17 Jan. 2012 [arxiv: 1112.2212v2 [nucl-th]].
- [24] Ch. Chen, Y. Lu, D. Binosi, C. D. Roberts, J. R. Quintero, J. Segovia, Rhys. Rev. D **99**, 034013 (2019), [arXiv:1811.08440v1[nucl-th]].
- [25] G. Ramalho, D. Melkinov, 3 Mar 2018 [arXiv:1703.03819v2 [hep-ph]].
- [26] G. Ramalho, M. T. Pena, 10 Mar 2020 [arxiv: 2003.04850v1 [hep-ph]].
- [27] I. Aznauryan, V. Braun, V. Burkert, S. Capstick, R. Edwards, I. C. Cloet, M. Giannini and T. S. H. Lee et al., [arXiv:0907.1901[nucl-th]].
- [28] V. I. Mokeev et al., Phys. Rev. C **93**, 025206 (2016) [arXiv:1509.05460 [nucl-ex]].
- [29] V. I.Mokeev et al., [CLAS Collaboration], Phys. Rev. C **86**, 035203 (2012), arXiv:1205.3948 [nucl-ex]].
- [30] A. Qattan, J. Arrington, 9 Dec. 2012 [arXiv:1209.0683v2 [nucl-ex]].
- [31] D. O. Riska, G. E. Brown, Nucl. Phys. A **679** (2001) 577-596.
- [32] I. G. Aznauryan et al. [CLAS Collaboration], Phys. Rev. C **80**, 055203 (2009) [arXiv:0909.2349[nucl-ex]].
- [33] G. Ramalho, K. Tsushima, Phys. Rev. D **81** (2010) 074010[arXiv:1002.3386[hep-ph]].
- [34] D. Drechsel, S. S. Kamalov and L. Tiator, Eur.Phys. J. A **34**, 69 (2007)[arXiv:0710.0306[nucl-th]].
- [35] L. Tiator, D. Drechsel, S. S. Kamalov and M. Vanderhaeghen, Chin. Phys. C **33**, 1069 (2009)[arXiv:0909.2335[nucl-th]].
- [36] M. M. Dalton et al., Phys.Rev. C **80**,015205 (2009) [arXiv:0804.3509[hep-ex]].
- [37] L. Tiator and M. Vanderhaeghen, Phys. Lett. B **672**, 344 (2009)[arXiv:0811.2285[hep-ph]].
- [38] J. Beringer et al. [Particle Data Group Collaboration], Phys. Rev. D **86**, 010001 (2012).

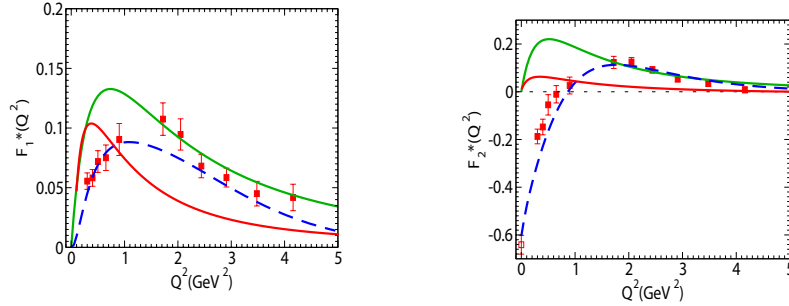


FIG. 1: $N + \gamma^* \rightarrow R(1440)$ transition Dirac and Pauli form factors (red lines) is compared with CLAS experimental data (squares with error bars) [32], MAID fit (dashed lines) [37] and valence quark contributions (solid lines) [33].

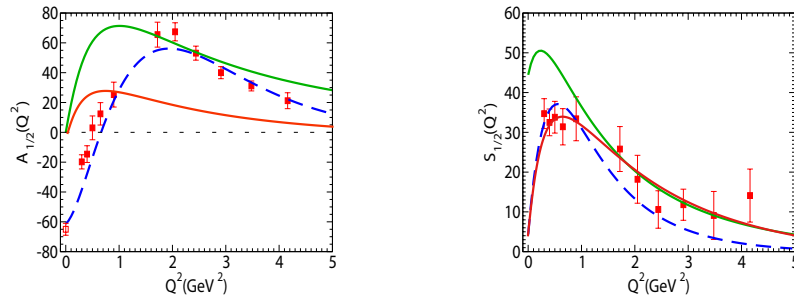


FIG. 2: $N + \gamma^* \rightarrow R(1440)$ transition $A_{1/2}(Q^2)$ and $S_{1/2}(Q^2)$ helicity amplitudes in units of $10^{-1/2} GeV^{-1/2}$ (red lines) is compared with CLAS experimental data (squares with error bars) [32], MAID fit (dashed lines) [37] and valence quark contributions (green solid lines) [33] are also shown.

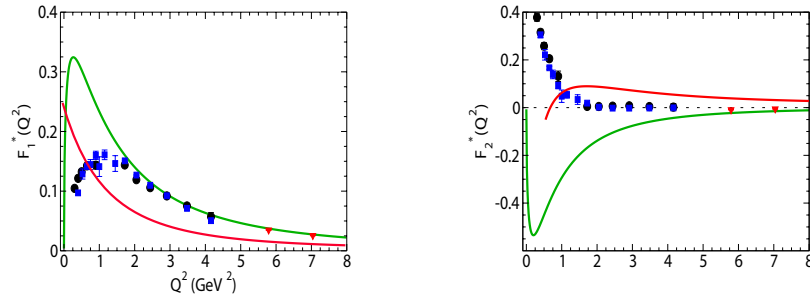


FIG. 3: Results for the $N + \gamma^* \rightarrow R(1535)$ transition Dirac and Pauli form factors (red lines) is compared with CLAS experimental data (full circles) [32], MAID (full squares) [34,35], JLab/Hall C (triangles) [36] and the semirelativistic approximation (green thick solid line) [4].

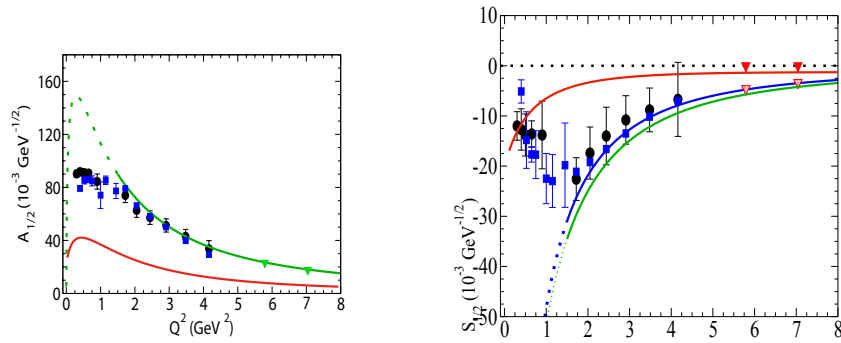


FIG. 4: Results for the $N + \gamma^* \rightarrow R(1535)$ transition $A_{1/2}(Q^2)$ and $S_{1/2}(Q^2)$ helicity amplitudes in units of $10^{-1/2} GeV^{-1/2}$ (red lines) is compared with CLAS experimental data (full circles) [32], MAID (full squares) [34,35], JLab/Hall C (triangles) [36], PDG (empty squares) [38] and the semirelativistic approximation (green thick solid line) [4].

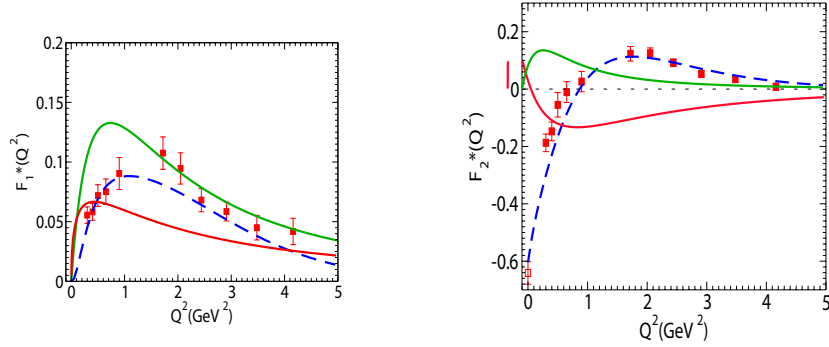


FIG. 5: $N + \gamma^* \rightarrow R(1710)$ transition transition Dirac and Pauli form factors (red lines) compared with CLAS experimental data (squares with error bars) [32], MAID fit (dashed lines) [37] and nonrelativistic quark model (green lines) [7].

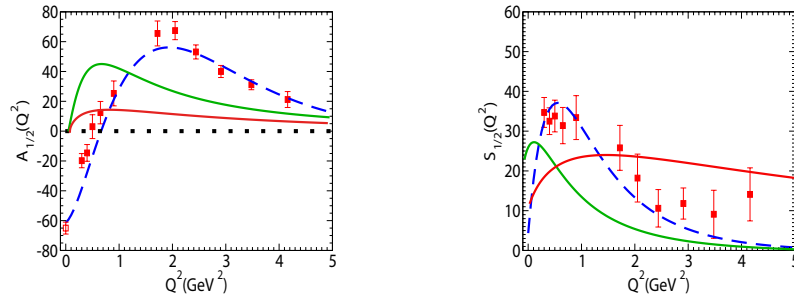


FIG. 6: $N + \gamma^* \rightarrow R(1710)$ transition $A_{1/2}(Q^2)$ and $S_{1/2}(Q^2)$ helicity amplitudes in units of $10^{-1/2} GeV^{-1/2}$ (red lines) is compared with CLAS experimental data (squares with error bars) [32], MAID fit (dashed lines) [37] and nonrelativistic quark model (green lines) [7].